ELSEVIER

Polymer 44 (2003) 1757–1763

polymer

www.elsevier.com/locate/polymer

Mesoscopic simulation of polymer–solvent phase separation: linear chain behaviour and branching effects

Roland E. van Vliet, Huub C.J. Hoefsloot, Piet D. Iedema*

Department of Chemical Engineering, University of Amsterdam, Nieuwe Achtergracht 166, 1018 WV Amsterdam, The Netherlands

Received 21 December 2001; received in revised form 30 December 2002; accepted 30 December 2002

Abstract

Recently, a method was presented to model phase separation behaviour of polymer–solvent mixtures around the lower critical solution temperature using dissipative particle dynamics (DPD) [Macromol Theory Simul 9 (2000) 698]. In the current article, a refined version of this method is described, yielding good agreement with the classic Flory–Huggins model. However, the great advantage of DPD, over such classical theories, is its ability to incorporate structural properties without additional parameters. This will be demonstrated on the case of branched polymers, for which DPD correctly predicts the cloud point pressure lowering experimentally observed.

Keywords: Flory–Huggins model; Dissipative particle dynamics; Branching

1. Introduction

One of the most important steps in a solution polymerisation process is the separation of solvents and impurities from the polymer. As the currently applied technique of steam stripping can be very energy-intensive (e.g. Gutowski et al. [2]), many alternatives have been proposed to improve this part of the process, both from an environmental and economical viewpoint.

In 1960, Freeman and Rowlinson [3] observed that a miscible polymer solution will separate into a polymer-rich phase and a solvent-rich phase if the temperature or pressure of the system approaches the critical temperature or pressure of the solvent. Since this discovery, many authors (e.g. Anolick and Slocum [4], Caywood [5], Irani et al. [6], McHugh and Guckes [7] and Seckner et al. [8]) have proposed that forcing the single-phase polymer solution to split into two equilibrium liquid phases may offer a better purification method.

Using classical thermodynamics, many polymer–solvent demixing phenomena can be described. This is, however, mostly on a steady-state basis, whereas knowledge of dynamic behaviour would offer better understanding of the liquid–liquid separation process and give rise to a more optimal design. Furthermore, the incorporation of structural properties, like branches, is not easily done and generally requires additional experimental and data-fitting effort.

In 1992, Hoogerbrugge and Koelman [9] proposed a new simulation technique referred to as dissipative particle dynamics (DPD). This particle-based method combines several aspects of molecular dynamics (MD) and lattice-gas automata. The particles or 'beads' represent 'fluid packages' or groups of particles that move according to Newton's equations of motion and interact dissipatively through simplified force laws. Hoogerbrugge and Koelman showed that their DPD algorithm obeys the Navier–Stokes equations. In 1995, the original scheme was modified by Español and Warren [10], in order to obtain a proper thermal equilibrium.

DPD can solve a variety of polymer-related problems, such as dynamics of confined polymers [11], microphase separation of block co-polymers [12] and polymer rheology [13] and melting [14]. Earlier work [1] showed that the typical occurrence of a lower critical solution temperature (LCST) curve could also be modelled using DPD. In the present article a quantitative comparison with the classical Flory–Huggins (FH) theory for polymer solutions is made. It will be shown that DPD essentially is a continuous version of this often-used lattice model. However, the effect of the molecular structure of polymers is not incorporated in the FH model. In a case study on the branching effect of

* Corresponding author. Tel.: +31-20-525-6484; fax: +31-20-525-5604.
E-mail address: piet@its.chem.uva.nl (P.D. Iedema).

0032-3861/03/$ - see front matter © 2003 Elsevier Science Ltd. All rights reserved.
doi:10.1016/S0032-3861(03)00023-5

polymers on the LCST curve, it will be shown that the influence of molecular structure on the liquid–liquid separation behaviour follows naturally from the DPD model, in which respect it is superior to the FH theory.

2. Polymer thermodynamics

2.1. Introduction

The phase behaviour of pseudo-binary polymer solutions can be described by the classification proposed by Scott and Van Konynenburg [15].

Fig. 1 depicts the phase diagram for a binary mixture that shows Type III phase behaviour, which is typical for many polymer–solvent systems. The pure component liquid–vapour boundaries end in the critical points. However, the liquids are not miscible at all temperatures. A liquid–liquid–vapour (LLV) line is present at temperatures lower than the critical temperature of either component. The LLV line ends in the upper critical end point (UCEP), the point at which one of the liquid phases becomes critically identical with the vapour phase, in the presence of the other liquid phase. The upper critical solution temperature (UCST) line, which begins at the UCEP and exhibits a slightly negative slope, represents the transition from two liquid phases to a single liquid phase with increasing temperature. The occurrence of the UCST curve is usually ascribed to enthalpic interactions between the mixture components, which are relatively insensitive to pressure changes for constant densities.

Furthermore, it can be seen that the branch of the critical mixture curve, which starts at the critical point of the component with the higher critical temperature, intersects a region of liquid immiscibility at the LCST. At temperatures below the LCST, a region of immiscibility again appears. The occurrence of the LCST curve is due to the large differences in the thermal expansion of the solvent and the polymer. As the solution is heated or the system pressure is reduced, the solvent expands at a much faster rate than the polymer so that the dissolution of the polymer in the solvent is associated with a large decrease in the change of entropy of mixing. The entropy decrease occurs as solvent molecules are forced to condense around the polymer to dissolve it. Eventually the loss in entropy in forming a single phase is so large that the Gibbs free energy of mixing becomes positive and the solution separates into two phases.

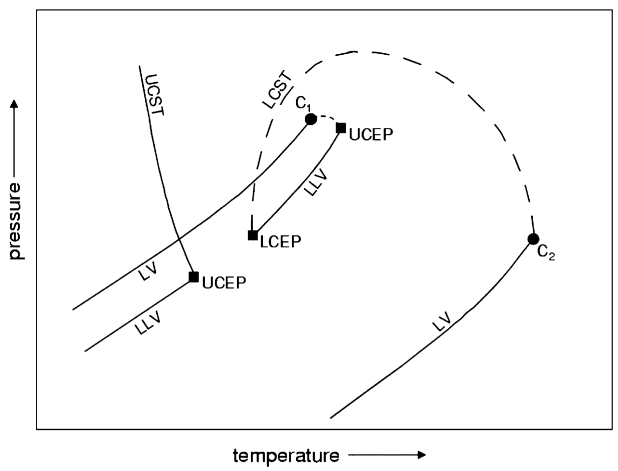

Fig. 1. Schematic pressure–temperature phase diagram of a binary mixture showing Type III phase behaviour.

From an industrial view point, the LCST curve is of more interest than the UCST curve as it can be concluded from experimental results that the UCST curve lies in the very low temperature (or even cryogenic) region, which is technically and economically not attractive.

2.2. Basic Flory–Huggins theory

Although many theories and models have been proposed to describe polymer–solvent thermodynamic behaviour, ranging from simple lattice based theories to equation of state models and statistical mechanics approaches (for an overview, see, e.g. Wohlfarth [16] and Case and Honeycutt [17]), the well-known FH theory is still applied in many cases, due to its simplicity and its ability to predict and classify several experimentally determined trends. In this paragraph, a short description of this model will be given as a prelude to the verification of the mesoscopic modelling technique as applied in this paper.

The FH theory [18] is the classical theory for calculating the free energy of mixing. In this theory, it is assumed that each (small) molecule of a mixture occupies one site on a lattice. By assuming that a polymer consists of a series of connected small molecules, the model can be expanded to polymer containing mixtures.

The ideal entropy of mixing ΔS of a binary system consisting of small molecules of equal size can be expressed as

$$-\frac{\Delta S}{NR} = x_1 \ln x_1 + x_2 \ln x_2 \tag{1}$$

where R is the universal gas constant, N the total number of moles and x_1 and x_2 are the mole fractions of components 1 and 2. However, for polymer systems, the mole fraction is a rather useless quantity as the number of chain molecules is decades smaller than monomeric mixtures at a comparable number of base units. In 1941, a theory on the effect of connectivity in polymer systems was published by Staverman and Van Santen [19], Huggins [20] and Flory [21]. For a binary solution the entropy of mixing is

$$-\frac{\Delta S}{NR} = \frac{\Phi_1}{m_1}\ln \Phi_1 + \frac{\Phi_2}{m_2}\ln \Phi_2 \tag{2}$$

where m_i is the number of segments (with molar volume V_L) of molecule i. The concentration variables are transformed to $\Phi_i = x_i/\sum_i x_i$ with $\sum_i \Phi_i = 1$ and can be considered as volume fractions. For non-interacting systems the free

enthalpy of mixing ΔG is defined as

$$\frac{\Delta G}{NRT} = \frac{\Delta S}{NR} \tag{3}$$

where T represents the absolute temperature.

Fig. 2 shows ΔG as a function of Φ_2 for three binary systems: an ideal low molecular weight mixture ($m_1 = 1$ and $m_2 = 1$), a polymer solution ($m_1 = 1$ and $m_2 > 1$) and a polymer mixture ($m_1 > 1$ and $m_2 > 1$). The $\Delta G(\Phi_2)$ curves are all concave upwards and have no inflection points which means that ideal mixtures (and athermic macromolecular mixtures) not can demix, as the coexistence of two separate phases will always correspond to a higher free energy compared to a single homogeneous phase. In order to describe separations into two or more liquid phases Eq. (2) needs to be extended, so that the equation describes $\Delta G(\Phi_2)$ curves which are partly negative and exhibit two or more inflection points. This can be done most easily be introducing an interaction term according to Van Laar ($g \times \Phi_1 \Phi_2$) with the interaction parameter g:

$$\frac{\Delta G}{NRT} = \frac{\Phi_1}{m_1} \ln \Phi_1 + \frac{\Phi_2}{m_2} \ln \Phi_2 + g(T, P, \Phi_2)\Phi_1 \Phi_2 \tag{4}$$

In Fig. 3, a typical free energy composition curve is shown as calculated with Eq. (4). Partial immiscibility is found at volume fractions Φ_1' and Φ_2'. If the locus of the points of the two phases that share a double tangent is extrapolated to the temperature-composition diagram, the binodal curve can be constructed. This so-called cloud point curve defines the limits of miscibility in the system. A homogeneous phase is stable if the volume fraction of component 2 is smaller than Φ_1' or larger than and Φ_2'. At intermediate compositions any single phase is thermodynamically unstable. The inflexion points define the spinodal or shadow curve under the binodal curve. In between the binodal and spinodal curve a metastable region is found. Finally, the point where the

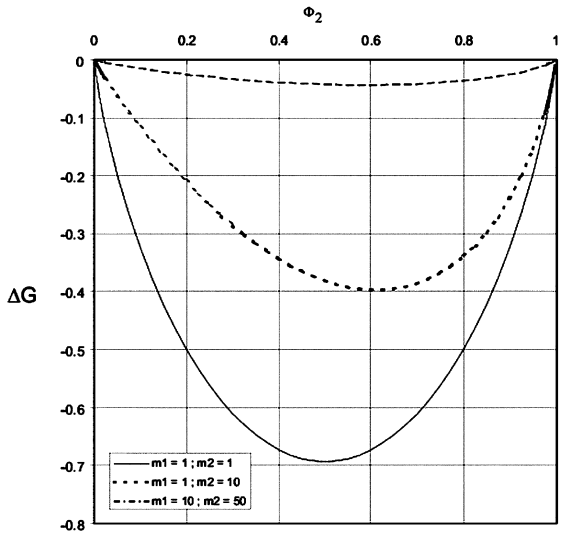

Fig. 2. ΔG as function of Φ_2 for three binary systems.

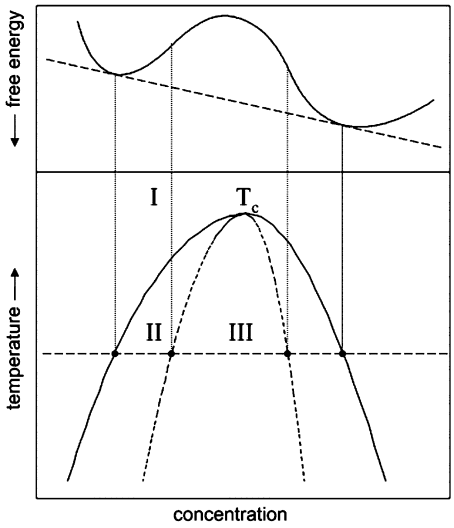

Fig. 3. Upper diagram: free energy composition curve. Lower diagram: extrapolation of free energy minima and inflection points to produce binodal and spinodal curves. Area II is the metastable region and area III is the unstable region. T_c is a UCST. Area I is the one-phase region.

inflection points merge, the critical temperature T_c can be defined above which the homogenous phase is stable.

The above-mentioned relationships allow calculation of the temperature-composition phase diagram based on the interaction parameter g (more commonly known as χ) only. If the concentration-dependency of g is not taken in consideration, the spinodal condition can be calculated from

$$\frac{1}{m_1 \Phi_1} + \frac{1}{m_2 \Phi_2} - 2g = 0 \tag{5}$$

and the critical volume fraction and critical interaction parameter are obtained from

$$\Phi_{2_c} = \frac{1}{(1 + \sqrt{(m_2/m_1)})} \tag{6}$$

$$g_c = \frac{1}{2}(1 + \sqrt{(m_2/m_1)})^2 \tag{7}$$

The most common assumed form for g is as follows:

$$g(T) = g_0 + \frac{g_1}{T} \tag{8}$$

The sign of parameter g_1 determines whether Eq. (8) describes UCST(+) or LCST(−) behaviour. The pressure dependence of g is usually incorporated in the g_0 and g_1 terms using some sort of power law form:

$$g_i = g_{i,1} + g_{i,2}P + g_{i,1}P^2 \tag{9}$$

However, other relationships have been proposed by several authors.

3. Dissipative particle dynamics

3.1. Model equations

In the DPD simulation method a set of particles moves according to Newton's equations of motion and interacts dissipatively through simplified force laws (e.g. Groot and Warren [22]). If the masses of all particles are taken equal to 1, the time evolutions of the positions ($\mathbf{r}_i(t)$) and impulses ($\mathbf{p}_i(t)$) are given by

$$\frac{\mathrm{d}\mathbf{r}_i}{\mathrm{d}t} = \mathbf{v}_i(t), \quad \frac{\mathrm{d}\mathbf{v}_i}{\mathrm{d}t} = \mathbf{f}_i(t) \tag{10}$$

The force acting on the particles is a combination of three contributions:

$$\mathbf{f}_{ij}^{\mathrm{C}} = \sum_{j \neq i} (\mathbf{F}_{ij}^{\mathrm{C}} + \mathbf{F}_{ij}^{\mathrm{D}} + \mathbf{F}_{ij}^{\mathrm{R}}) \tag{11}$$

The conservative force is a soft repulsion given by

$$\mathbf{F}_{ij}^{\mathrm{C}} = \begin{cases} a_{ij}\left(1 - \dfrac{r_{ij}}{r_{\mathrm{c}}}\right)\hat{\mathbf{r}}_{ij} & (r_{ij} > r_{\mathrm{c}}) \\ 0 & (r_{ij} \leq r_{\mathrm{c}}) \end{cases} \tag{12}$$

where a_{ij} is the maximum repulsion between particle i and j, $\mathbf{r}_{ij} = \mathbf{r}_i - \mathbf{r}_j$, $r_{ij} = |\mathbf{r}_{ij}|$, $\mathbf{r}_{ij} = \mathbf{r}_{ij}/|\mathbf{r}_{ij}|$, and r_{c} is the cut-off radius. The other two forces are the dissipative and the random force, which are given by

$$\mathbf{F}_{ij}^{\mathrm{D}} = -\gamma\omega^{\mathrm{D}}(r_{ij})(\hat{\mathbf{r}}_{ij}\cdot\mathbf{v}_{ij})\hat{\mathbf{r}}_{ij}, \qquad \mathbf{F}_{ij}^{\mathrm{R}} = \sigma\omega^{\mathrm{R}}(r_{ij})\theta_{ij}\hat{\mathbf{r}}_{ij} \tag{13}$$

where $\mathbf{v}_{ij} = \mathbf{v}_i - \mathbf{v}_j$, ω^{D} and ω^{R} are r-dependent weight functions tending to zero for $r = r_{\mathrm{c}}$ and θ_{ij} is a randomly fluctuating variable with zero mean and unit variance. Español and Warren [10] showed that the weight functions and constants in Eq. (13) can be chosen arbitrarily, but should obey

$$[\omega^{\mathrm{R}}(r_{ij})]^2 = \omega^{\mathrm{D}}(r_{ij}), \qquad \sigma^2 = 2k_{\mathrm{B}}T\gamma \tag{14}$$

where k_{B} is the Boltzmann constant and T is the temperature of the fluid. The equations are solved using the modified velocity-Verlet algorithm as described by Groot and Warren. The random force weight function is defined as $1 - r/r_{\mathrm{c}}$, where $r_{\mathrm{c}} = 0$.

3.2. Spring force

In the DPD model, individual atoms or molecules are not represented directly by the particles but they are grouped together into beads. These beads represent local 'fluid packages' able to move independently. Polymers are represented by bead-strings of 5–30 beads, which turns out to be sufficient to reproduce the typical chain-like nature of polymers. In DPD, the connection in a polymer string is established by adding a spring force between the beads. Thus, beads can be interconnected to highly complex topologies, e.g. branched architectures.

Choosing the correct spring force deserves closer examination. Two types of spring force have been applied in literature. Groot and Warren advocated the use of the harmonic spring:

$$F_{ij}^{\mathrm{spring}} = K\cdot\mathbf{r}_{ij} \tag{15}$$

where K is the spring constant. In this way the mean distance between two consecutive chain beads is governed by the spring force and the repulsive interaction. The value of the spring constant is chosen such that the mean spring distance corresponds to the distance found at the maximum of the pair correlation function of the polymer beads when the spring constant is equal to zero. However, in this manner connected beads are not prevented from being located far more than r_{c} apart. This is highly undesirable as hydrodynamic interaction between beads within the same polymer chain is lost and it would be easy for polymer chains to cross each other without ever experiencing any mutual interaction. This is comparable to neglecting the Zimm corrections [23] on the dynamical chain behaviour as predicted by the Rouse model [24]. Of course, a stiffer spring could be modelled by choosing a larger spring constant, but, essentially, this would also imply an increase in the density of the polymers.

In order to overcome these problems, the Fraenkel spring, as applied by Schlijper et al. [13], is used in our simulations:

$$F_{ij}^{\mathrm{spring}} = K\cdot(r_{ij} - r_{\mathrm{eq}})\cdot\hat{\mathbf{r}}_{ij} \tag{16}$$

Here r_{eq} is the equilibrium spring distance (chosen as $r_{\mathrm{eq}} = \dfrac{1}{\sqrt[3]{\rho}}$), which is independent from the stiffness of the polymer spring. The spring constant is determined by simulating polymer chains at the relevant conditions for demixing simulations. The distance between two consecutive beads in the polymer chains is sampled for several spring constants. The spring constant value at which 98% of the cumulative spring distance distribution lies within one is chosen as the correct value.

3.3. Model refinement for improved LCST description

Previously, the DPD model could predict UCST behaviour but was unable to describe LCST phase behaviour. In view of the similar deficiency of the FH theory in describing LCST behaviour, we applied an analogous strategy [1] to solve this problem. Where, according to the modified FH theory the temperature and pressure dependence is incorporated in the g-parameter, in DPD we ascribed such dependencies to the interaction parameter a_{ij}. To this end, the inter-species repulsion parameter was made a monotonically increasing function of temperature. A pressure effect was introduced by changing both the inter- and intra-species repulsion parameter with pressure. The intra-species repulsion

parameter is linearly and stepwise decreased, while simultaneously the value of the inter-species repulsion parameter is increased, thereby increasing the overall system pressure. In this way, both a pressure drop and a temperature increase effectuated a widening of the demixing gap. It was shown that true Type III phase behaviour can be mimicked by the DPD model.

However, it has already been noted, that the temperature-dependency of the repulsion parameter should probably be mapped in a more sophisticated manner than a linear relationship, similar to the temperature-dependency of the parameter in the FH-theory (Eqs. (8) and (9)). Therefore, in this work, the DPD inter-species interaction parameter is chosen as

$$a_{ij}(T,P) = s + \frac{u + v{\cdot}P}{k_B T} \tag{17}$$

whereas the intra-species interaction parameter is defined as

$$a_{ij}(T,P) = a_{jj}(T,P) = q{\cdot}P + r \tag{18}$$

Like Eq. (8), the sign of parameter determines whether UCST(+) or LCST(−) behaviour is described. The values of the variables (Table 1) are chosen such that the interaction parameters adopt values of the same order of magnitude as those reported in the previous work.

To make a quantitative comparison between DPD and FH, the results of FH calculations can be mapped onto the DPD data by applying a scaling factor c, which can be defined as

$$c = \frac{g}{(a_{ij} - a_{ii})} \tag{19}$$

When discussing the results of the simulations, values of found will be reported.

3.4. Simulation parameters

The system consisted of polymers with 30 beads per chain, connected by the aforementioned Fraenkel springs and dissolved in a solvent represented by single beads, with a total number of beads of 12,000. The polymer weight fraction amounted to 50%. The polymer–solvent system was placed in a simulation box with dimensions $40 \times 10 \times 10 r_c$. By choosing a rectangular shaped box, the formation of a stable planar interface is enhanced. As periodic boundary conditions are applied on all sides of the simulation box, more than one polymer–solvent interface is formed. In a density profile plot this shows as a polymer slab enclosed on both sides by solvent particles. A full simulation covers an interface formation period of 80,000 time steps, followed by a period of 50,000 steps where the density profile was sampled at an interval rate of 100 steps. In Table 2, all other DPD model parameters are listed.

Table 1
Repulsion parameter variable values for LCST behaviour

Parameter	Value
q	1.25
r	−7.25
s	60
u	30
v	−6

4. DPD and Flory–Huggins compared

The refined model has been tested by calculating the density profiles of linear polymer–solvent at three different temperatures for several pressures. From these results the concentration of polymer and solvent in the two liquid phases can be calculated and a pressure-composition diagram, as shown in Fig. 4, can be constructed. From the figure, a few conclusions can be drawn. First of all, the asymmetrical shape of the dissolution curve is clearly visible, which is so typical for polymer–solvent liquid–liquid separations. Furthermore, both with decreasing pressure and with increasing temperature the demixing gap widens, indicating LCST behaviour.

In order to compare the DPD simulation technique to classical theories, the demixing calculations have also been performed using the FH model. All parameters were kept identical to the DPD simulation. Thus, the same temperature, pressure, polymer concentration and chain length were applied. Furthermore, the pressure and temperature dependencies of the DPD repulsion parameter were transferred to the FH g-parameter variables (Eqs. (8) and (9)). In Table 3, the g-parameter values can be found.

From Fig. 4, it can be seen that very good agreement exists between DPD and FH. No DPD results are available in the vicinity of the critical point, due to excessive calculation times. However, it is clear that a discrepancy between DPD and FH exists near the critical point. Probably, this can be ascribed to the fact that FH is a lattice-based theory as opposed to the off-lattice approach of DPD. A more quantitative comparison can be made by mapping the FH results onto the DPD simulations. On theoretical grounds, Groot and Warren found the aforementioned scaling factor (Eq. (19)) possesses a value of 0.286 for $\rho = 3$, $g > 3$ and $k_B T = 1.0$. In this work, scale factors of 0.2346, 0.2652 and 0.2880 for $k_B T = 2.0$, 3.0 and 4.0

Table 2
DPD simulation parameters

Parameter	Value
ρ	3.00
σ	3.35
γ	3.00
δt	0.04
r_c	1.0
K	150.00
r_{eq}	0.693

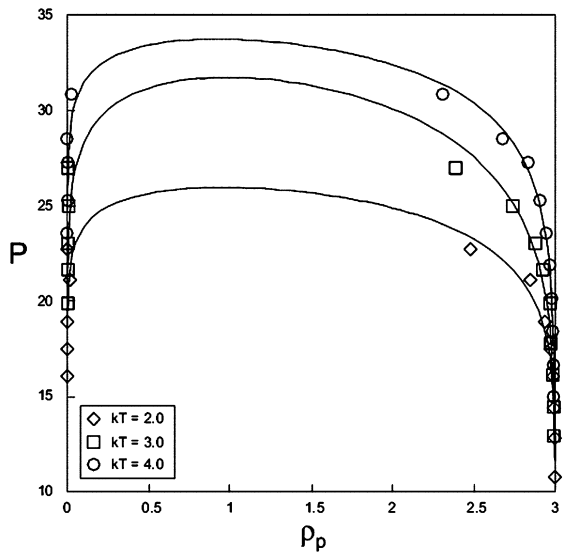

Fig. 4. Pressure-composition phase diagram for the model linear polymer–solvent system calculated with DPD as compared to the FH calculations. ρ_c is the concentration of the polymer.

were obtained, not far from the theoretical value. A small temperature effect in the relationship between the DPD interaction parameter and the FH g-parameter seems to exist. This may be attributed to deficiencies in both FH and DPD models. These are probably due to the fact that the deviation between FH and DPD near the critical point becomes more important at higher temperatures as a result of the increased motion of the molecules. Also, the pressure dependence introduced in the intra-species interaction parameter (Eq. (18)) is, apparently, overpronounced as compared to the FH results.

5. Case study: branching effect

To illustrate the advantage of DPD over many classical theories and especially the FH model in accounting for molecular structure, simulations are performed on branched polymers instead of linear chains. Experimental work has revealed that the cloud point pressures decreased with increasing branchedness of the polymer (see, e.g. Chen et al. [25], De Loos et al. [26], Whaley et al. [27] and Han et al. [28]). The solubility is seen to decrease, which may be attributed to lower effective polymer interaction energy. This would, in turn, increase the similarity between the polymer chains and the small solvent molecules. Partly, these effects may be related to the much smaller radius of gyration of branched molecules compared to linear chained molecules of the same molecular weight.

Table 3
FH model parameter values for LCST behaviour

Parameter	Value
$g_{0,1}$	67.25
$g_{0,2}$	−1.25
$g_{1,1}$	30
$g_{1,2}$	−6

It is impossible to describe the branching effect with the FH theory purely on a structural basis, as molecular shapes do not play a role in this model. Kleintjens et al. [29] introduce a interaction energy term and an empirical entropy correction in the definition for the g-parameter. Likewise, in the well-known SAFT equation of state, the effect of branching can be introduced only by adjusting the branch segment energy parameter for each structural change in the polymer [28].

The incorporation of molecular structure is straightforward in DPD, since any structure can be modelled, varying from linear chains to highly branched molecules. We have performed a simulation with a branched polymer constructed as a linear backbone of 18 beads and three 4-bead side chains. By again choosing a 30-bead molecule, like in the linear polymer simulation, any change in results not can be ascribed to differences in molecular weight. The same parameters were used as in the linear chain simulation. However, we choose a lower temperature $k_B T = 1.0$, as the temperatures of the previous simulations gave rise to intensive diffusion. The mobility of the polymers then is at such levels where even the linear chains, with the larger radius of gyration, have no difficulty penetrating the solvent phase and any branching effect is lost.

In Fig. 5, the pressure-composition diagrams for both the linear and the branched chain polymers are shown. At first, it can be seen clearly that the asymmetrical phase separation behaviour is retained. Interestingly, the branched polymer possesses a critical point at a lower pressure, which agrees to the experimental findings mentioned above. As expected, we could relate this lowering to the reduction of the radius

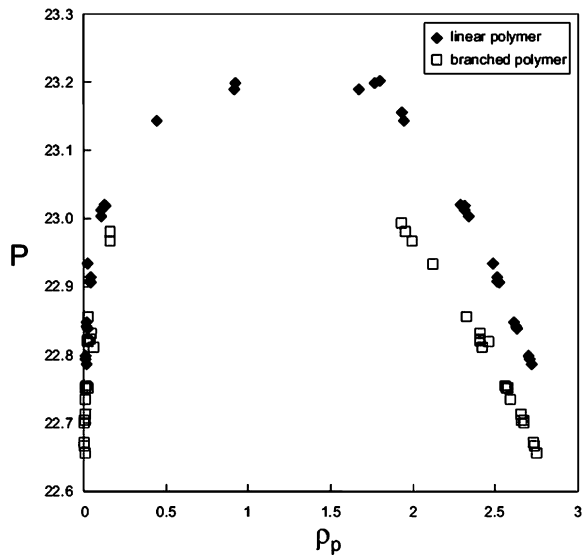

Fig. 5. Pressure-composition diagram of the linear polymer–solvent system compared to the branched polymer–solvent system as calculated with DPD. ρ_c is the concentration of the polymer.

of gyration in the branched polymers. This reduces the repulsive forces between the solvent molecules and polymer segments, while increasing the mobility of the polymers. Both effects lead to a better solubility of the polymers.

6. Conclusions

In this article a refined version of the temperature- and pressure-dependent DPD repulsion parameter is presented, enabling the DPD to simulate true Type III phase behaviour and predict LCST phase separation. Very good agreement is obtained with the classical FH theory. The calculated scale dependence between the two models agrees with earlier findings. Furthermore, we have demonstrated the power of DPD to describe molecular structure effects on thermodynamics. The influence of branching on the phase behaviour of polymer systems was correctly predicted by introducing the branched structure in the chain. This is a remarkable advantage over classical theories, that require certain fit parameters to correct for structural effects. In future work, the relationship between molecular structure and the branching effect will be studied in more detail as well as the influence of this relation on the dynamics of the liquid–liquid separation.

We thus conclude that DPD is a high potential simulation technique for thermodynamics. In relatively simple systems it yields good agreement to classical models. However, in more complex systems, that are unattainable for classical theories without additional parameters, DPD appears to predict trends remarkably well. Subsequent mapping of DPD parameters to physical ones then is the major practical test. As another strong point of DPD, it should be noted that it covers both thermodynamic equilibrium issues well as dynamics. The latter naturally opens the way to investigate flow effects on phase separation, which is the topic of present research.

Acknowledgements

The authors would like to thank Sander Willemsen for the fruitful discussions and comments. Financial support for REVV provided by NWO-CW is gratefully acknowledged.

References

[1] Van Vliet RE, Hoefsloot HCJ, Hamersma PJ, Iedema PD. Macromol Theory Simul 2000;9:698.
[2] Gutowski TG, Suh NP, Cangialose CG, Berube M. Polym Engng Sci 1983;23:230.
[3] Freeman PI, Rowlinson JS. Polymer 1960;1:20.
[4] Anolick, C., Slocum, E.W. US Patent 3,726,843, 1973.
[5] Caywood, S.W. US Patent 3,496,135, 1971.
[6] Irani, C.A., Cozewith, C., Kassegrande, S.S. US Patent 4,319,021, 1982.
[7] McHugh MA, Guckes TL. Macromolecules 1985;18:674.
[8] Seckner AJ, McClellan AK, McHugh MA. AIChE J 1988;34:9.
[9] Hoogerbrugge PJ, Koelman JMVA. Europhys Lett 1992;19:155.
[10] Español P, Warren P. Phys Rev E 1995;52:1734.
[11] Kong Y, Manke CW, Madden WG, Schlijper AG. Int J Thermophys 1994;15:1093.
[12] Groot RD, Madden TJ. J Chem Phys 1998;108:8713.
[13] Schlijper AG, Manke CW, Madden WG, Kong Y. Int J Mod Phys C 1997;8:919.
[14] Willemsen SM, Visser DC, Hoefsloot HCJ, Iedema PD. J Comp Phys 2000;162:385.
[15] Scott RL, Van Konynenburg PB. Discuss Faraday Soc 1970;49:87.
[16] Wohlfart C. Makromol Chem, Theor Simul 1993;2:605.
[17] Case FH, Honeycutt JD. Trends Polym Sci 1994;2:259.
[18] Flory PJ. Principles of polymer chemistry. Ithaca: Cornell University Press; 1953.
[19] Staverman AJ, Van Santen JH. Rec Trav Chim 1941;60:60.
[20] Huggins ML. J Chem Phys 1941;9:440.
[21] Flory PJ. J Chem Phys 1941;9:660.
[22] Groot RD, Warren PB. J Chem Phys 1997;107:4423.
[23] Zimm BH. J Chem Phys 1956;24:269.
[24] Rouse PE. J Chem Phys 1953;21:1272.
[25] Chen SJ, Banaszk M, Radosz M. Macromolecules 1995;28:1812.
[26] De Loos ThW, Poot W, Lichtenthaler RN. J Supercrit Fluids 1995;8:282.
[27] Whaley PD, Winter HH, Ehrlich P. Macromolecules 1997;30:4887.
[28] Han SJ, Lohse DJ, Radosz M, Sperling LH. Macromolecules 1998;31:2533.
[29] Kleintjens LA, Schoffeleers HM, Koningsveld R. Ber Bunsenges Phys Chem 1997;81:980.